

荷重 Hadamard 變換의 映像符號化

(Weighted Hadamard Transform Image Coding)

李 門 浩*

(Moon Ho Lee)

要 約

本 論文에서는 荷重 Hadamard 變換을 정의했고(WHT) 또한 효율적인 高速 WHT의 알고리즘을 연구 하였다. WHT는 Hadamard 變換과 같이 映像信號를 처리 하였으며 WHT는 Hadamard 變換의 空間 周波 數 영역에 荷重을 주어 送信했고 受信時에는 中心의 高周波 영역을 무시하였다. 이렇게 할때 信號對 雜 音比와 映像의 돋보임이 Hadamard 變換에 비해 向上되었다.

Abstract

In this paper, we have defined the Weighted Hadamard Transform (WHT) and developed efficient algorithms for the fast computation of the WHT. The WHT is applied to digital image processing and compared with Hadamard Transform (HT). We have weighted at the center spatial frequency domains of the Hadamard Transform and transmitted a image and then center high frequencies are neglected at the receiving.

The WHT of signal to noise ratio (SNR) and image quality are enhanced than the HT.

I. Introduction

The application of discrete orthogonal transforms for image representation and compression is well-known [1], [2]. A much-investigated method, due to the ease and efficiency of its implementation, is based on the Hadamard transform (HT).

In this paper, we present a modification to the HT, which we call the Weighted Hadamard transform (WHT). This method retains much of the simplicity of HT, but offers better quality of representation over the central region of the image [3]. The scheme was motivated by two factors. First, the main features of many images are placed in the center of the field of view of the TV camera. Second, it is known that the human visual system (HVS) is

most sensitive to the mid spatial frequencies [3],[6],[12],[13],[14]. The WHT emphasizes the spatial and frequency domain features in these regions.

The paper is organized as follows. First, in the next section the WHT is introduced and recursive relations for the generation of the transform matrix is presented. The fast WHT algorithm similar to a fast HT method is derived for both the forward and inverse transforms. Second, examples are presented that compare the effects of the quantization errors on the representation of images by the HT and the WHT as well as the quality of data compression by neglecting high-frequency Hadamard and Weighted Hadamard coefficients. The data compression examples are merely presented to compare the HT and the WHT techniques. Third, we have made a hardware realization of the WHT that has used some shift register and digital adder on the weighted mid-spatial domain.

*正會員, 全北大學校 電子工學科

(Dept. of Elec. Eng., Chonbuk National Univ.)

接受日字: 1986年 9月 15日

II. The Weighted Hadamard Transform

Let the Hadamard and Weighted Hadamard matrices of order $N=2^n$ be denoted by $[H]_N$ and $[WH]_N$ respectively. The WHT of an $N \times 1$ vector $[f]$ and an $N \times N$ (image) matrix $[g]$ are given as in the case of the HT by

$$\begin{aligned} [F] &= [WH]_N [f] \quad \text{and} \\ [f] &= [WH]_N^{-1} [F] \end{aligned} \quad (1)$$

$$\begin{aligned} [G] &= [WH]_N [g] [WH]_N \quad \text{and} \\ [g] &= [WH]_N^{-1} [G] [WH]_N^{-T} \end{aligned} \quad (2)$$

The lowest-order WH matrix is of order four and is defined together with its inverse by

$$[WH]_4 \triangleq \begin{bmatrix} 1 & 1 & 1 & 1 \\ 1 & -2 & 2 & -1 \\ 1 & 2 & -2 & -1 \\ 1 & -1 & -1 & 1 \end{bmatrix} \quad (3)$$

$$[WH]_4^{-1} = \frac{1}{8} \begin{bmatrix} 2 & 2 & 2 & 2 \\ 2 & -1 & 1 & -2 \\ 2 & 1 & -1 & -2 \\ 2 & -2 & -2 & 2 \end{bmatrix} \quad (4)$$

This choice weighting was dictated, to a large extent, by the requirements of hardware simplicity and error performance results.

As with the Hadamard matrix, a recursive relation governs the generation of higher order WH matrices. Thus

$$[WH]_8 = [WH]_4 \otimes [H]_2 \quad (5)$$

$$[WH]_N \triangleq [WH]_{N/2} \otimes [H]_2 \quad (6)$$

where \otimes is the Kronecker product.

$[H]_2$ is the lowest-order Hadamard matrices. [1], [5].

$$[H]_2 = \begin{bmatrix} 1 & 1 \\ 1 & -1 \end{bmatrix} \quad (7)$$

The kernel of $[WH]$ is followed by HT as shown

$$[H]_4 = \begin{bmatrix} + & + & + & + \\ + & - & + & - \\ + & + & - & - \\ + & - & - & + \end{bmatrix} \quad (8)$$

$$[H]_8 = \begin{bmatrix} + & + & + & + & + & + & + & + \\ + & - & + & - & + & - & + & - \\ + & + & - & - & + & + & - & - \\ + & - & - & + & + & - & - & + \\ + & + & + & + & - & - & - & - \\ + & - & + & - & - & + & - & + \\ + & + & - & - & - & - & + & + \\ + & - & - & + & - & + & + & - \end{bmatrix} \quad (9)$$

We have weighted at the center frequency domain of the Hadamard transform. It emphasizes frequency domain features in these regions. Some initial results of this paper were presented at the [3], [11], [14].

III. Fast Weighted Hadamard Transform (FWHT) Algorithm

A fast Hadamard transform (FHT) algorithm was outlined in 1937 by Yates. In 1958 and 1969, Good and Pratt et al describes matrices decomposition techniques which can be implemented to perform the HT with the $N \log_2 N$ operation. [1], [2], [4], [9].

We now present a fast algorithm for the WHT which is intimately related to the fast HT (FHT) algorithm [2], [4]. The FHT can be derived by decomposing $[H]_N$ into a product of n sparse matrices, each having rows with only two non-zero elements. In order to develop a similar algorithm for the WHT, define a coefficient matrix $[WC]_N$ by

$$[WC]_N = [H]_N [WH]_N. \quad (10)$$

Since $[H]_N^{-1} = \frac{1}{N} [H]_N$, we have from (10) that

$$[WH]_N = \frac{1}{N} [H]_N [WC]_N. \quad (11)$$

It is shown that $[WC]_N$ is a sparse matrix with at most two non-zero elements per row and column. Therefore, the FWHT is simply the FHT followed by a sparse operator $\frac{1}{N} [WC]_N$.

To show the sparseness of $[WC]_N$ we start by computing the lowest order $[WC]$, i.e. $[WC]_4$.

From (10), we have

$$[WC]_4 = \begin{bmatrix} 1 & 1 & 1 & 1 \\ 1 & -1 & 1 & -1 \\ 1 & 1 & -1 & -1 \\ 1 & -1 & -1 & 1 \end{bmatrix} \begin{bmatrix} 1 & 1 & 1 & 1 \\ 1 & -2 & 2 & -1 \\ 1 & 2 & -2 & -1 \\ 1 & -1 & -1 & 1 \end{bmatrix} = \begin{bmatrix} 4 & 0 & 0 & 0 \\ 0 & 6 & -2 & 0 \\ 0 & -2 & 6 & 0 \\ 0 & 0 & 0 & 4 \end{bmatrix} \quad (12)$$

Clearly $[WC]_4$ is sparse. Using the expansion properties of the Hadamard and Weighted Hadamard matrices, (10) can be written as

$$\begin{aligned} [WC]_N &= ([H]_{N/2} \otimes [H]_2) ([WH]_{N/2} \otimes [H]_2) \\ &= ([H]_{N/2} [WH]_{N/2}) \otimes ([H]_2 [H]_2) = \\ &= [WC]_{N/2} \otimes (2I_2), \end{aligned} \quad (13)$$

where $[I]_2$ is the 2×2 identity matrix. Since $[WC]_4$ is symmetric and has at most two non-zero elements in each row, it clearly follows from (13) that the same is true for $[WC]_8$ and hence for any $[WC]_N$, $N=2^k$, $k=2,3,4, \dots$

a. Forward Fast Weighted Hadamard Transform

The WH matrix decomposition is of the form of the Kronecker products of $[H]_2$ matrices and successively lower order WH matrices.

The forward fast Weighted Hadamard transform (FFWHT) is given formulas as shown

$$\begin{aligned} [WH]_8 &= [H]_8^{-1} [WH]_8 = \frac{1}{8} [([H]_4 \otimes [H]_2) ([WC]_4 \otimes 2I_2)] \\ &= \frac{1}{8} [([H]_4 [WC]_4) \otimes 2[H]_2 [I]_2] \\ &= \frac{1}{8} [([H]_4 [WC]_4) \otimes 2[H]_2] \end{aligned} \quad (14)$$

Where $[WH]_N$ represents the matrices of order N . The recursive relationship is given by the expression

$$[WH]_N = \frac{1}{N} ([H]_{N/2} [WC]_{N/2}) \otimes 2[H]_2 \quad (15)$$

This decomposition leads very clearly to a sparse matrix factorization of the WH matrix.

b. Reverse Fast Weighted Hadamard Transform

The reverse FWHT may be formulated in a similar fashion as the FWHT. First we note that

$$[WC]_N^{-1} = [WC]_{N/2}^{-1} \otimes \frac{1}{2} [I]_2 \quad (16)$$

Equation (16) can be shown to be true by multiplying $[WC]_N^{-1}$ in (16) by the expression for $[WC]_N$ given in (13). From (16) and the sparseness and symmetry of $[WC]_N^{-1}$ it follows that $[WC]_N^{-1}$ is also symmetric and sparse. Furthermore, using (15), we have

$$[WH]_N^{-1} = N [WC]_N^{-1} [H]_N^{-1} \quad (17)$$

But $[WC]_N$ and $[H]_N^{-1} = \frac{1}{N} [H]_N$ are both symmetric with a symmetric product. Thus,

$$\begin{aligned} [WH]_N^{-1} &= [H]_N [WC]_N^{-1} \\ &= ([H]_{N/2} [WC]_{N/2}^{-1}) \otimes \frac{1}{2} [H]_2 \end{aligned} \quad (18)$$

Equation (18), with the exception of the scale factor $\frac{1}{N}$, is of the same form as (15). Consequently, it signifies a fast algorithm for the inverse of $[WH]_N$ composed of FHT followed by the operation of the sparse matrix $x [WC]_N^{-1}$.

We know that the $[WC]$ is always symmetric matrix. i.e.

$$[WC]_N [WC]_N^{-1} = [I]_N \quad (19)$$

The proof of (19) is very simple. Using the algebra of Kronecker products [2], we have

$$\begin{aligned} [WC]_N [WC]_N^{-1} &= ([WC]_{N/2} \otimes 2I_2) ([WC]_{N/2}^{-1} \otimes 1/2I_2) \\ &= ([WC]_{N/2} [WC]_{N/2}^{-1}) \otimes ([I]_2 [I]_2) = \\ &= [I]_N \end{aligned} \quad (20)$$

The proof is complete.

The WHT_w makes a decomposition of sparse matrices as below: [4]

$$\begin{bmatrix} + & + & + & + \\ + & - & + & - \\ + & + & - & - \\ + & - & - & + \end{bmatrix} = \begin{bmatrix} + & \circ & + & \circ \\ \circ & + & \circ & + \\ + & \circ & - & \circ \\ \circ & + & \circ & - \end{bmatrix} \begin{bmatrix} + & + & \circ & \circ \\ + & - & \circ & \circ \\ \circ & \circ & + & + \\ \circ & \circ & + & - \end{bmatrix} \quad (21)$$

$$\begin{bmatrix} X_2(0) \\ X_2(1) \\ X_2(2) \\ X_2(3) \end{bmatrix} = \begin{bmatrix} 1 & 0 & 1 & 0 \\ 0 & 1 & 0 & 1 \\ 1 & 0 & -1 & 0 \\ 0 & 1 & 0 & -1 \end{bmatrix} \begin{bmatrix} X_1(0) \\ X_1(1) \\ X_1(2) \\ X_1(3) \end{bmatrix} \begin{bmatrix} X_3(0) \\ X_3(1) \\ X_3(2) \\ X_3(3) \end{bmatrix}$$

$$= \begin{bmatrix} 1 & 1 & 0 & 0 \\ 1 & -1 & 0 & 0 \\ 0 & 0 & 1 & 1 \\ 0 & 0 & 1 & -1 \end{bmatrix} \begin{bmatrix} X_2(0) \\ X_2(1) \\ X_2(2) \\ X_2(3) \end{bmatrix}$$

$$\begin{bmatrix} X_4(0) \\ X_4(1) \\ X_4(2) \\ X_4(3) \end{bmatrix} = \begin{bmatrix} 4 & 0 & 0 & 0 \\ 0 & 6 & -2 & 0 \\ 0 & -2 & 6 & 0 \\ 0 & 0 & 0 & 4 \end{bmatrix} \begin{bmatrix} X_3(0) \\ X_3(1) \\ X_3(2) \\ X_3(3) \end{bmatrix} \quad (22)$$

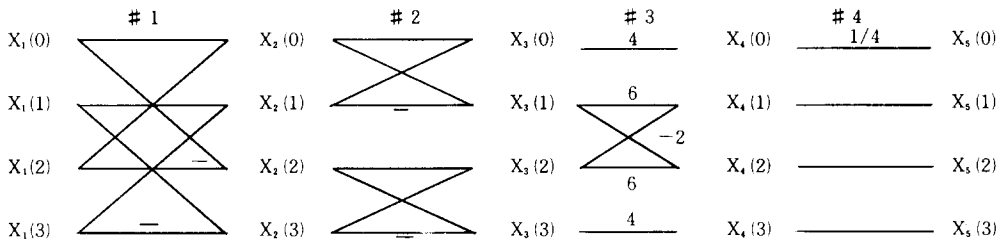
The signal flow graphs for WHT₄ based on (21), (22) are shown in Fig. 1.

The FFWHT₈ signal flow graph illustrated in Fig. 2.

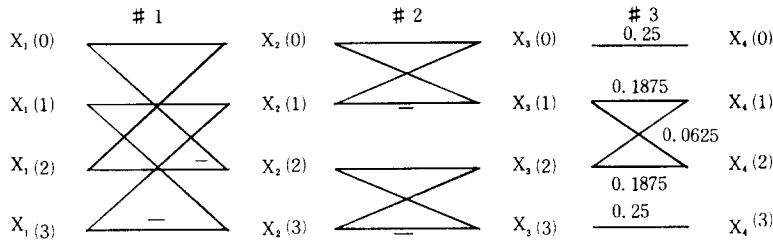
There is a comparison of computing numbers between the FHT and FWHT in table 1.

Table 1. Comparison of computing numbers of FHT and FWHT.

form	HT	fast HT	WHT		fast WHT	
	Add	Add	Add	Mult.	Add	Mult.
4 × 4	12	8	12	4	10	6
8 × 8	56	24	56	16	28	12
16 × 16	240	64	240	24	72	24
EQ.	N(N-1)	N × n	N(N-1)	2 ⁿ⁻¹	$\frac{N}{2}(2n+1)$	6 × 2 ⁿ⁻¹



(a) FFWHT



(b) RFWHT

Fig. 1. Fast weighted Hadamard transform signal flow graph, N=4. Iteration number (#) = log₂N+1.

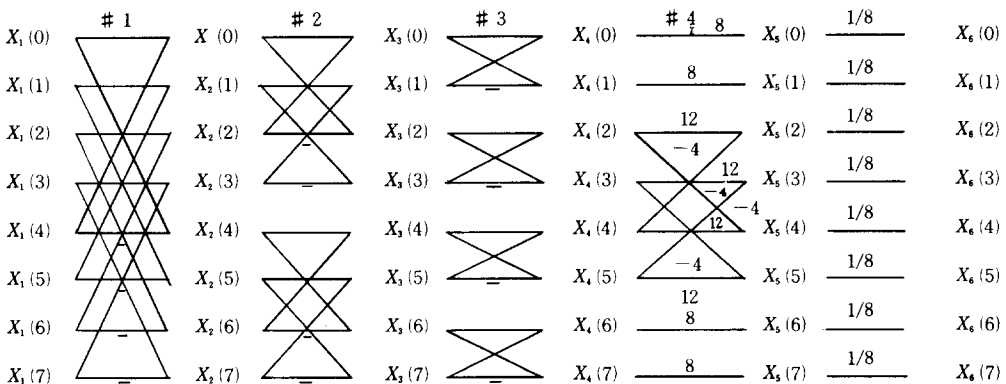


Fig. 2. FFWHT signal flow graph, N=8.

The FWHT algorithm is shown as below in Fig. 3.

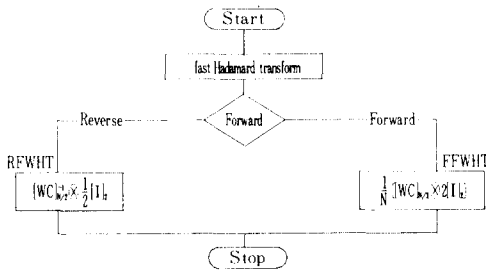


Fig. 3. FWHT flow chart.

IV. Image Processing

The WHT of image processing is shown in Fig. 4.

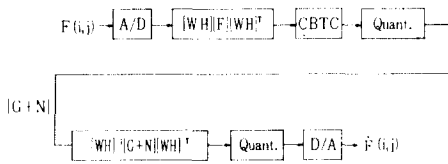


Fig. 4. WHT image processing

The original image, shown in Picture 1, is a 64x64 pixel and 8-bit uniformly quantized representation of a girls face. This image is used as the input to the transform algorithm.

First of all, the human visual response to spatial frequencies is nonuniform and the mid-spatial frequencies are emphasized more than the low and high spatial frequencies. [6],[10].

The use of particular properties of the HVS in image coding is referred to as psychovisual coding. [15].

We have weighted in the center spatial frequency domains and transmitted a image and then adopted center block truncation coding (CBTC). This transform conserve the signal energy in the transform domain, but typically most of this energy is concentrated in relatively few samples which area usually the lower frequency samples.

Several years ago, block truncation coding

(BTC) was developed by Delp and Mitchell. [7].

In this paper, we will present a modified BTC scheme which is called CBTC.

The scheme is simple: first, the two-dimensional transform image divides into two blocks. One is an edge boundary pixel (4x4) that is retained without coding, and the other is a large center block, a subpicture 8x8 block, where the 8x8 blocks are coded individually.

Second, each subpicture 8x8 block has a two level signal representation.

Let X_1, X_2, \dots, X_m be the value of the transformed image.

Then by Delp [7], the first and second sample moments and the sample variance have, respectively:

$$\bar{X} = \frac{1}{m} \sum_{i=1}^m X_i \tag{23}$$

$$\overline{X^2} = \frac{1}{m} \sum_{i=1}^m X_i^2 \tag{24}$$

$$\sigma^2 = \overline{X^2} - \bar{X}^2 \tag{25}$$

As with the design of any one bit quantizer, we find a threshold, X_{th} , and two output levels, a and b:

if

$$\bar{X}_i \geq X_{th} \text{ output} = b \tag{26}$$

$$\bar{X}_i < X_{th} \text{ output} = a \tag{27}$$

for $i = 1, 2, \dots, m$.

Let q be the number of X_i 's greater than \bar{X}_{th} ($=\bar{X}$) then to preserve \bar{X} and $\overline{X^2}$

$$m\bar{X} = (m-q) a + qb \tag{28}$$

$$m\overline{X^2} = (m-q) a^2 + qb^2 \tag{29}$$

Solving for a and b

$$a = \bar{X} - \bar{\sigma} \sqrt{\left(\frac{q}{m-q}\right)} \tag{30}$$

$$b = \bar{X} + \bar{\sigma} \sqrt{\left(\frac{q}{m-q}\right)} \tag{31}$$

The reconstructed image block is transmitted by calculating a and b from equations (30) (31) and assigning these new values to pixels in accordance with the bit plane. The transmitting image is linear quantized, inverse two-

dimensional processing is done, and then the original signals are replicated.

We confirmed a center block which divides into subpicture block size (8×8). This center block comes out more data compressed and enhanced subjective image quality more than any other block size.

The objective image fidelity criteria are the MSE, SNR and SNR peak and then we look for the input and output image. An interesting relationship between SNR and subjective picture quality is that they are proportional.

Let a value of i and j in the range of 0, 1, ..., N-1 then the error between an input image and the corresponding output image is

$$e(i, j) = \hat{F}(i, j) - F(i, j) \tag{32}$$

The mean square error (MSE) is

$$MSE = \frac{1}{N^2} \sum_{i=0}^{N-1} \sum_{j=0}^{N-1} [\hat{F}(i, j) - F(i, j)]^2 \tag{33}$$

An output signal has an input signal plus error that is

$$\hat{F}(i, j) = F(i, j) + e(i, j) \tag{34}$$

The SNR is given by

$$SNR = \left[\frac{\sum_{i=0}^{N-1} \sum_{j=0}^{N-1} \hat{F}^2(i, j)}{\sum_{i=0}^{N-1} \sum_{j=0}^{N-1} [\hat{F}(i, j) - F(i, j)]^2} \right]^{1/2} \tag{35}$$

The peak value of $\hat{F}(i, j)$ is the total dynamic range of the output image

$$SNR_{peak} = \{ [\text{peak values of } F(i, j)]^2 / MSE \}^{1/2} \tag{36}$$

The MSE, SNR, and SNR peak between the input and the reconstructed image is computed for various compression data in Table 2.

V. WHT Hardware Implementation

One dimensional WHT₄ coefficients for a sequence of input signal sample values $\{f_1, f_2, f_3, f_4\}$ are $[F_1, F_2, F_3, F_4]$ that is

$$[F_1, F_2, F_3, F_4]^T = [WH_4] [f_1, f_2, f_3, f_4]^T \tag{37}$$

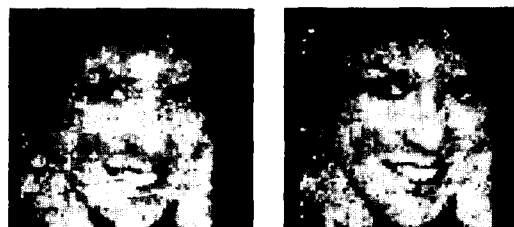
Table 2. MSE, SNR at the HT and WHT

Transform	MSE	SNR	SNR _{peak}	picture
HT	21.451	33.454	229.545	2
WHT	10.055	48.787	189.251	
HT	16.068	38.635	213.273	3
WHT	8.545	53.047	178.978	
HT	12.794	43.298	198.281	4
WHT	7.564	56.385	173.661	
HT	12.006	44.704	196.084	5
WHT	6.012	63.100	162.847	



(a) original girl (525×525) (b) 8bit uniform quantization (64×64)

Picture 1. Original girl face



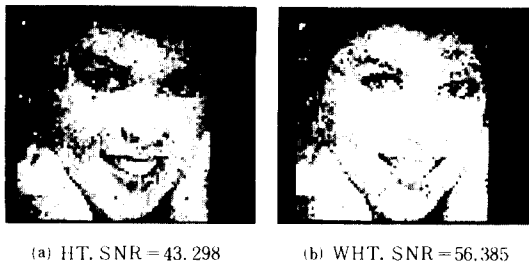
(a) HT. SNR = 33.454 (b) WHT. SNR = 48.787

Picture 2. 1 bits/pixel

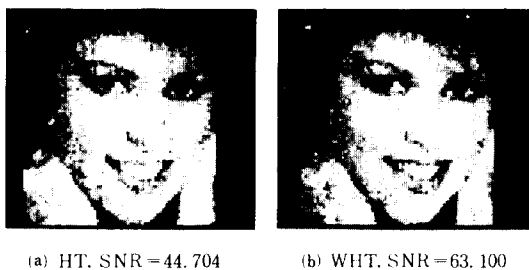


(a) HT. SNR = 38.635 (b) WHT. SNR = 53.047

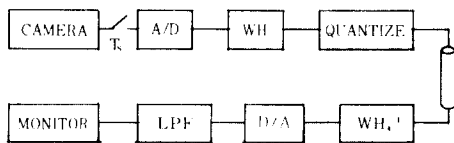
Picture 3. 2.64 bits/pixel



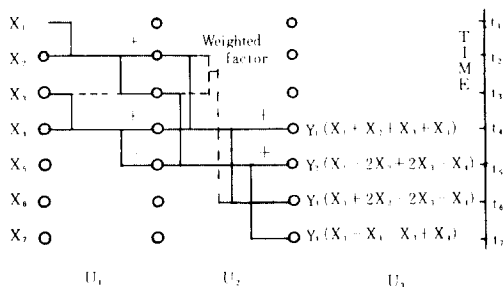
Picture 4. 4.17 bits/pixel.



Picture 5. Quantize noise at the transform domain.



(a) System block diagram



(b) Calculation algorithm

Fig. 5. WHT₄ system block diagram and its calculation algorithm.

This real time cascaded unit algorithm of WHT₄ is shown in Fig. 5.

The WHT₄ has HT₄ and weighted factor units. HT₄ consists of two unit and each unit has shift registers (TTL 7496), data selectors (TTL 74157), inverters (“NOT”circuit for each bit to make one’s complement for subtraction) and full adders (TTL 7483).

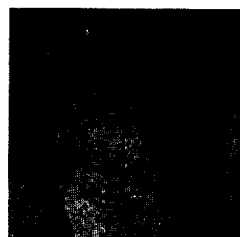
In order to make the 2’s complement effectively, one is added to the least significant bit of the full adder in the case of subtraction.

The overall system is designed as a synchronous master clock system. The input signal data are memorized at the shift register. Add and subtract operation are performed in the full adder according to the clock cycle change:

In until the operation which are $(X_1+X_2)=D_1$, $(X_1-X_2)=D_2$, $(X_3+X_4)=D_3$ and $(X_3-X_4)=D_4$ are performed at t_2, t_3, t_4 and t_5 respectively. The operations that $D_1+D_3, D_2+D_4, D_1-D_3$ and D_2-D_4 are done in unit2 at t_4, t_5, t_6 and t_7 respectively. The weighted factor unit is similar to one of HT₄ units. In weighted factor unit, the operations of X_2-X_3 and $-X_2+X_3$ are performed and the transformed coefficients are delayed for a time being. The transformed coefficient $-X_2+X_3$ is added to the D_2+D_4 at t_5 and X_2-X_3 is added to the D_1-D_3 at t_6 .



(a) A/D · D/A (b) HT



(c) WHT

Fig. 6 Real time processing of grandfather.

In the experiment, the sampling frequency is 4 MHz and the signal coded at 4 bits/sample. The reconstructed images are shown in Fig. 6.

We can see the noise of block transform in Fig. 6(b) and lower electric field noise of TV signal in (C).

6. Conclusion

The signal to noise ratio at the receiving units has been improved by employing the proposed WHT rather than the HT to enhance subjective image quality.

We have developed center block truncation coding methods for data compression, fast Weighted Hadamard transform, and a simplified hardware realization of the shift register and adder (subtractor).

References

- [1] W.K. Pratt, J. Kane, H.C. Andrews, "Hadamard transform image coding", *Proc. IEEE* vol. 57, Jan. 1969, pp. 58-68.
- [2] N. Ahmed, K.R. Rao, "Orthogonal transform digital signal processing", *Springer-Verlag*, 1975, pp. 141-143.
- [3] J.O. Yoon, O. Ch. Ham, M.H. Lee, "Image data processing by weighted Hadamard transform", *KIEE Proc.*, vol. 6, no. 1, July 1983.
- [4] M.H. Lee, M. Kaveh, "Fast Hadamard transform based on simple matrix factorization", *IEEE* vol. ASSP-34, no.6, Dec. 1986.
- [5] R.C. Gonzalez, P. Wintz, "Digital image processing", *Addison-Wesely pub.* 1977.
- [6] Douglas J.G., "The role of human visual models in image processing", *IEEE, proc.* vol. 69, no. 5, May 1981.
- [7] E.J. Delp, O.R. Mitchell, "Image compression using block truncation coding",

IEEE vol. Com-29, no. 9, Sept. 1979 pp. 1335-1342.

- [8] Takahiko Fukinuki and M. Miyata, "Intraframe image coding by cascaded Hadamard transform", *IEEE* vol. com-21, no. 3, Mar. 1973.
- [9] K.R. Rao, M.A. Narasiman, K. Revulmi, "Image data processing by Hadamard-Haar transform", *IEEE* vol. C-24, no. 9, Sept. 1975, pp. 888-896.
- [10] Manfred Tasto, Paul A. Wintz, "Image coding by adaptive block quantization", *IEEE*, vol. Com-19, no. 6, Dec. 1971, pp. 857-871.
- [11] M.H. Lee, D.Y. Kim, "Weighted Hadamard transformation for S/N ratio Enhancement in image transmission", *IEEE ISCAS Proc.*, May 1984, pp. 65-68.
- [12] S. Ericsson, "Frequency weighted interframe hybrid coding", *Telecomm. Theory Electrical Engineering, Royal Institute of Technology, Sweden, Technical Report*, Jan. 1984.
- [13] N.B. Nill, "A Visual model weighted cosine transform for image compression and quality assessment", *IEEE Trans. Com-33*, no. 6, June 1985, pp. 551-557.
- [14] M.H. Lee, Y.S. Lim, "The center-weighted Hadamard transform," *IEEE Trans. Comm.* to be submitted 1987.
- [15] J.I. Mannos, D.J. Sakrison, "The Effects of a Visual Fidelity Criterion on the Encoding of Image" *IEEE* vol. Information Theory 20. no. 4, pp. 525-536. July 1974.

Acknowledgement

This work was supported in part by the Korean Science and Engineering Foundation.